COMPLETELY CONSISTENT 'NO-CHARGE' PHEMT MODEL INCLUDING DC/RF DISPERSION

C. J. Wei, Y. A. Tkachenko, J. Gering and D. Bartle

Alpha Industries Inc. 20 Sylvan Road, Woburn, MA 01801

Abstract — **A new large-signal PHEMT model based on independent fitting of DC currents, RF currents, and capacitances is developed. Unlike conventional models, it does not contain charge terms and therefore, avoids the problem of path-dependence in the charge-integration of capacitances. Similar consideration is given to the dispersion of conductances. Since each nonlinear element of the model corresponds to an element of the small-signal equivalent circuit, the model shows complete consistency over the bias range of the model's extraction. The model features accuracy and simplicity of extraction. It is especially useful for PHEMTs or FETs with dispersion.**

I. INTRODUCTION

Large-signal FET/PHEMT modeling has advanced to a mature stage. Various empirical and table-based models have been developed [1-7] and are widely used. High accuracy has been achieved for those devices that satisfy charge conservation and show insignificant dispersion. Several papers [10-12] have dealt with dispersion with limited success.

The major difficulty is that conventional large-signal models that fit DC IV and QV characteristics are often inconsistent with small-signal models. Small-signal models derived from large-signal models have different values from those extracted from S-parameters. The currents and charges obtained from integration of measured small-signal element values are normally not unique because of the integration path-dependence due to dispersion.

The new model proposed here, has several features. (1) It does not contain charge terms and all the elements are nonlinear currents, including capacitive currents. (2) RF conductance and RF-trans-conductance values are different from those at DC. (3) The nonlinear functions can be independently extracted from a table of bias-dependent small-signal element values. (4) The functions have high-order continuous derivatives. The first two features ensure complete consistency with conventional small-signal models, since they have an exact correspondence between the model elements. A small-signal model derived from a conventional large-signal model contains as many as four trans-capacitance elements that makes the above consistency very difficult. In the new model there is no ambiguity involved because there are no trans-capacitance terms, except for one that translates to a delay time in connection with Gm. The third feature simplifies the model extraction. Finally, the last feature ensures fast convergence and accurate two-tone simulations.

II. EQUIVALENT CIRCUIT MODEL

The charge terms in conventional models can be replaced with capacitive currents. Filicori, et. al. in their elegant paper [9], proved that any nonlinear circuit can be reduced to a network consisting of nonlinear resistances or current sources and linear capacitances.

For complete consistency, the current flowing into branch i, in addition to the DC terms, is divided into two classes of currents: conductive currents, such as drain currents Irf1 and Irf2, and capacitive currents $\sum_j C_{ij} \cdot dv_j/dt$, where i=j are local terms and i≠j are non-local terms, and v_j is the RF voltage across the j-th branch. To separate the DC V_{jo} from the instantaneous Vi and to create a voltage node dv_j/dt, the sub-circuits in Figure 1 are used. We denote Vg and Vd as instantaneous gate and drain voltages, and Vgo and Vdo as their DC components.

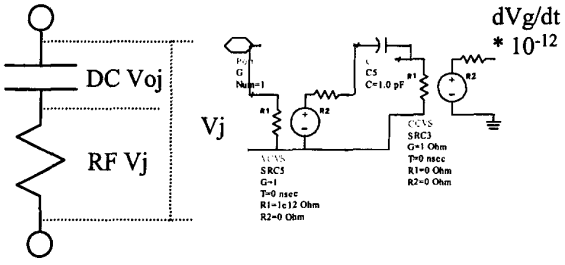

Figure 1. Sub-circuits to obtain DC Vjo, RF Vj and dVg/dt.

Figure 1 shows how to obtain the respective voltage sources. The DC component of a branch voltage is taken from the capacitance of a series-RC shunted across the branch, assuming RC>>1/f and R>1 Mohm. The dVj/dt is obtained in a slightly tricky manner. First apply the voltage Vj on a 1pF capacitance, and the current through the capacitance is exactly dVj/dt times the factor of 1e-12. Here, we use 1pF instead of a 1F to reduce the numerical

0-7803-7239-5/02/$10.00 © 2002 IEEE

error at high frequencies. Figure 2 shows the intrinsic part of the device model. The currents are expressed as

Ids_cap= Cm(Vg,Vd)·dVgs/dt+Cds(Vg,Vd)·dVds/dt,
Igd_cap=Cgd(Vg,Vd)·dVgd/dt, and
Igs_cap=Cgs(Vg,Vd)·dVgs/dt,

where Ids_cap, Igd_cap and Igs_cap are the capacitive currents flowing through branches D-S, D-G and G-S, respectively, and Cm=Gm·tau.

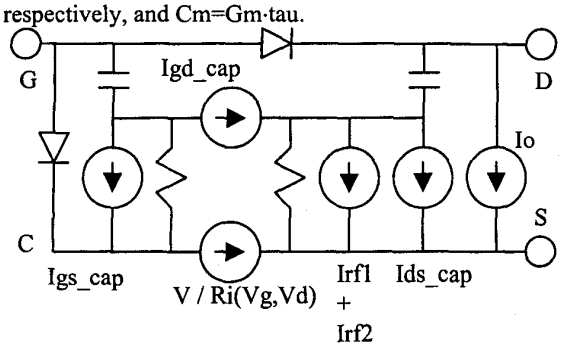

Figure 2. Intrinsic nonlinear currents of the model

Three current sources are combined to represent the DC and RF components. Io, the DC current, and Irf1 and Irf2, the RF conductive currents, are

Io=-Idc(Vg,Vd)+Idc(Vgo,Vd)+Idc(Vg,Vdo),
Irf1=Igm(Vg,Vd)-Igm(Vgo,Vd), and
Irf2=Igds(Vg,Vd)-Igds(Vg,Vdo),

where Igm and Igds are the D-S RF currents that fit the RF Gm and RF Gds, respectively. They are obtained by integrating Gm and Gds with respect to Vgs and Vds along different integration paths [8]. The arguments of all the functions are the instantaneous port voltages and DC voltages. The current in the C-S branch is also used, where C denotes the internal node at the gate-end of the channel. The CR circuits are aimed at separating the DC and RF parts of the currents.

Assuming a small deviation of the port voltages and neglecting the higher-order term, one finds that the currents have the following correspondence to the elements of the small-signal model: Igs_cap⇒Cgs, Igd_cap⇒Cgd, Ids_cap⇒Gm·τ+Cds, Irf1⇒Gm, and Irf2⇒Gds. The total current reduces to Idc when Vg=Vgo and Vd=Vdo. The derivatives of Itotal = Irf1+Irf2+Io with respect to Vg and Vd reduce to the RF trans-conductance and drain-source conductance, respectively.

Gm=∂Itotal/∂Vg=∂Igm/∂Vg
Gds=∂Itotal/∂Vd=∂Igds/∂Vd

The model elegantly separates the DC components from RF-components, which gives consistency with small-signal models and accurate modeling of dispersion. Moreover, the charge terms are eliminated altogether, making the model extraction much easier and faster.

III. Model Extraction

As in our previous work [4,5,7], the model has a thermal sub-circuit for modeling self-heating. The DC characteristics are defined as follows. (Refer to [4] for parameters *c* and *Cbk*.)

$$I_{ds} = Io\exp(-c\,P_{av})(1+\tanh((V_{gs}-V_{go})/V_{det}))$$

$$Io = \frac{Imax}{2}(1+\tanh\phi)(1+kVds)\tanh((a+\eta(0.95-V_{gs}))V_{ds})$$

$$\phi = P_1 x + P_2 x^2 + P_3 x^3$$

$$x = V_{ge} - V_{to} + V_{ds}\gamma$$

P_{av} is the average device power dissipation in operation with a thermal constant. The functions for RF Gm and RF Gds describe the respective derivatives with respect to Vgs and Vds using different sets of parameters.

The functions for Cgs are expressed as

$$C_{gs} = C_{gso} + C_{gsm}/(1+\exp(-(V_{gs}-V_{co})/V_{cd}))\text{ and}$$

$$C_{gsm} = \frac{Cmax}{2}(1+\tanh\phi)(1+kc(Vgs-Vk)),$$

where $\phi = C_1 x + C_2 x^2 + C_3 x^3$ and

$$x = V_{ds} - V_{cto}$$

The functions for calculating Cgd are given below.

$$C_{gd} = C_1 + \frac{(C_n - C_1)}{(1+e^{(-(V_{gs}-V_o)/V_{gd})})(1+e^{((V_{ds}-V_{do})/V_{dd})})}$$

$$C_1 = C_{p1} + (C_{f1} - C_{p1})/(1+\exp(-(V_{gs}-V_{c1})/V_{cd1}))$$

$$C_n = C_{pm} + (C_{fm} - C_{pm})/(1+\exp(-(V_{gs}-V_{c2})/V_{cd2}))$$

$$V_{dd} = a_1 + a_2(1-V_{gs})$$

These equations are adequate to fit the table-data for the measured capacitances as functions of the port voltages.

As an example, 6x200um and 40x100um, 0.5um gate-length, Alpha D-PHEMTs are used. For such large devices, a complex topology of the equivalent circuit would be required to account for distributed effects. Nevertheless, a conventional model topology is used, and therefore, self-heating and other dispersion effects cannot be ignored because of the big differences between DC Gm/Gds and RF Gm/Gds and also because charge conservation does not apply. The S-parameters are measured over a bias range from below pinch-off to forward gate biases and with Vds from 0 to 5 V. The small-signal models are extracted using in-house program

ALPHAEXT which features fast direct extraction with no optimization involved.

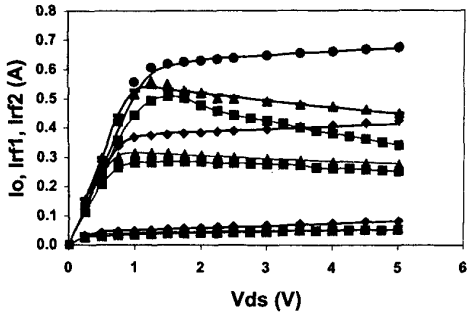

Figure 3. Measured (symbol) and fitted (line) dc IV, Igm and Igds. Vg=-0.8, 0 and 0.8 V. DC curves are squares, Igm curves are triangles, and Igds curves are diamonds.

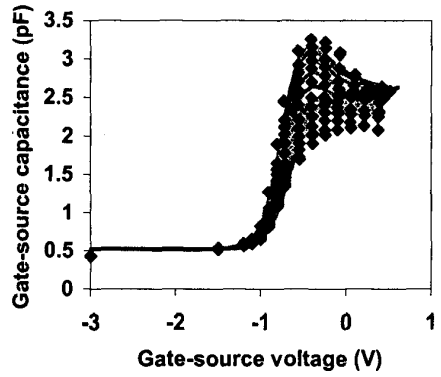

Figure 4. Fitted (line) and measured (symbol) Cgs as a function of Vgs and Vds.

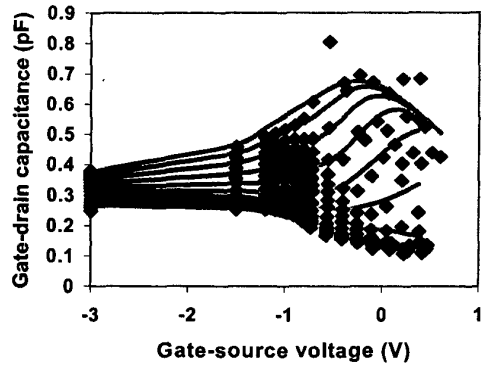

Figure 5. Fitted (line) and measured (symbol) Cgd as a function of Vgs and Vds.

Figure 3 plots the measured and fitted DC IV curves as well as the Igm and Igds curves at three Vg values. It is shown that the Igm curves deviate from the DC IV curves at higher gate voltages. The Igds curves are much different from both the Igm and the DC IV characteristics.

Figures 4 and 5 show very good fitting of Cgs and Cgd characteristics, respectively. Fitting of other parameter parameters is omitted here for the sake of brevity.

IV. MODELING RESULTS

To verify the consistency between the large-signal and small-signal models, S-parameter fitting is verified at various bias conditions. Figures 6 and 7 plot the modeled and measured S-parameters for the 6x200 um device at several bias points: Vg=0.7 V and -0.5 V and Vd=0.5 V (linear region), Vg=-1.5 V and Vd=4 V (below-pinch-off region), and Vg=-0.8 V and Vd=4 V (saturation region).

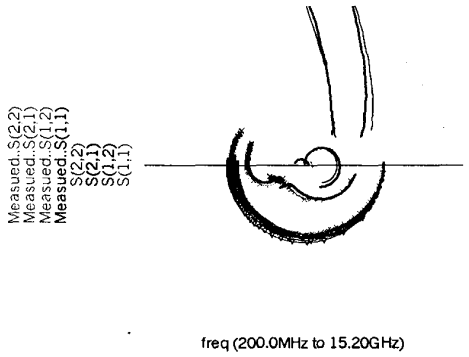

Figure 6. Model (line) verse measured (symbol) S11, S22, S12, and S21 at four typical bias-points

Based on the model extracted from the 6x200 um device, the model for a large 36x125 um device was developed by linearly scaling the internal elements and nonlinearly scaling the extrinsic elements. Figure 8 shows the modeled and measured power performance at f = 3.4 GHz, source reflection = $0.5\angle 179.2$, and load reflection = $0.57\angle 152.4$ and = $0.35\angle 15.9$ at the fundamental and second harmonic, respectively. The device is biased at Vg = -0.71 V and Vd=5 V. Very good agreement is achieved between the modeled and measured results.

It is noteworthy that the device is biased at Vd = 5 V, which is the upper end point of the bias range used for device characterization and model extraction. The voltage swing at high power drives can be as high as 11 V at the peak. Good agreement in the power performance prediction indicates that the equations used to fit the model parameters nicely extrapolate beyond the region of extraction.

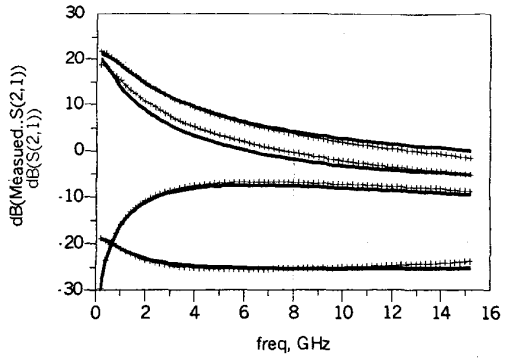

Figure 7. Model (line) vs measured (symbol) S21 in dB at four typical bias-points.

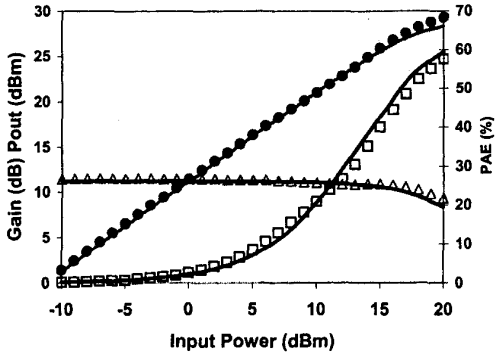

Figure 8. Simulated (line) vs measured (symbol) power performance of a 36x125 um PHEMT at f = 3.4 GHz, and Vd = 5V, quiescent drain current is Icq = 0.1 A.

V. CONCLUSION

A new MESFET/PHEMT model composed of only currents is developed. The new model is based on a one-to-one correspondence between the small-signal model elements and nonlinear functions of port voltages and therefore features consistency between the large-signal and small-signal models. Fitting of Cgd and Cgs is independent and does not require charge-conservation. Also, dispersion effects can be effectively handled since the RF Gds and RF Gm can be different from the DC Gds and DC Gm. The model is accurate, yet calculation-efficient. It is more complex and yet relatively simple to extract. At present, the model is empirical, but table-based models can be applied equally well. The model is especially useful for those devices, where dispersion and non-charge conservation are significant.

REFERENCES

1. W. Curtice, M.Ettenburg,"A nonlinear GaAs FET model for use in design of output circuit of power amplifiers," *IEEE Trans Microwave Theory & Tech,* vol.33, no.12,pp1383,1985
2. D. E. Root, S, Fan, and J. Meyer, "Technology-independent Large-signal FET Model: A measurement-based Approach to Active Device Modeling," 1991, *Proc. 15th ARMMS Conference*
3. I. Angelov, "Chalmers Nonlinear HEMT and MESFET model," *Report 26, Chalmers University of Technology,* ISSN 1103-4599
4. C. J. Wei, Y. A. Tkachenko, and D. Bartle, "An accurate large-signal model of GaAs MESFET which accounts for charge conservation, dispersion, and self-heating," *IEEE Trans Microwave Theory & Tech,* vol.11, pp.1638-, 1998
5. C. J. Wei, Y. A. Tkachenko, and D. Bartle, "A new analytic model for power E-mode PHEMTs and its optimum power operation," presented at IMOC'99, Rio-de-Janeiro, Aug.9-12,1999
6. Ph. Jansen, D. Schreurs, W. De Raedt, B. Nauwelaers, and M. Van Rossum, "Consistent small-signal and large-signal extraction techniques for heterojunction FETs," in IEEE Trans. on Microwave Theory and Tech., Vol. 43, No. 1, Jan. 1995, pp. 87-93.
7. C.J. Wei, J.W. Bao and J.C.M. Hwang, "Novel Experimentally-based Modeling for MESFET's Having Complex Dispersion Effects," *IEEE Workshop on Experimentally-Based FET Modeling & Related Nonlinear Circuit Design,* July 17-18,1997 Kassel, Germany, pp. 22.1-8
8. C. J. Wei, Y. A. Tkachenko and D. Bartle, "Novel approach to a consistent large-signal and small-signal modeling of power PHEMTs," *2001 APMC, Dec.3-6, Teipei*
9. M. C. Filicori and G. Vannini, "Mathematical Approach to Large-signal Modeling of Elecronic Devives," 1991, *Electronic Devices*, Vol.27, pp.357-359
10. K. Jeon, Y. Kwon, and S. Hong, "A Feequency Dispersion Model of GaAs MESFET for Large-Signal Applications," *IEEE Microwave and Guided Wave Letters,* vol. 7, no.3, pp.78-80, 1997
11. C. Camecho-Penalosa and C. S. Aitchison, "Modeling Frequency Dependence of Output Impedance of a Microwave NESFET at Low Frequency," Electronics Letters, Vol.21, pp.528-529, June 1985
12. V.I. Cojocaru and T.J. Brazil, "A Scalable General-Purpose Model for Microwave FET's Including the DC/AC Dispersion Effects,", IEEE Trans. On MTT, Vol.45, No.12, 1997
13. C.-J. Wei, Y.A. Tkachenko and D. Bartle, "Alpha Owned PHEMT Model and Its Verification by Load-Pull and Waveform Measurements," 2000-APMC, Sydney, Australia, Dec.2-6, 2000